A Wide-Band, High Isolation UHF Lumped-Element Ferrite Circulator

Hang Dong, Jacob R. Smith, and Jeffrey L. Young, *Fellow, IEEE*

***Abstract*—A novel, spiral trace topology for a lumped-element, ferrite circulator is demonstrated in this letter. By employing this new topology, along with various optimization methods, we achieve high isolation and wide bandwidth for UHF applications. Based on simulation data, circulator isolation of 30 dB or more is possible over the 245–355 MHz frequency range. The isolation response of a fabricated spiral trace circulator exceeds 30 dB, but over a shifted and wider frequency range of 260 to 390 MHz.**

***Index Terms*—Bandwidth, circulation impedance, isolation, lumped-element circulator.**

I. Introduction

THE basic theory of a lumped-element, crossover ferrite circulator for VHF and UHF applications was established by Konishi in 1965 [1]. In recent years, discussions on bandwidth optimization for a given isolation specification have received considerable attention, e.g., see [2]. A typical circulator consists of three parts, as depicted in Fig. 1: a) the crossover network, which is constructed by two fully saturated ferrite disks and three electrically isolated traces between them; b) the tuning elements C_0 and C_g, which set the center frequency of the device and impact device bandwidth [3]; c) the matching network components C_1 and L_1, which establish an impedance match with the load R_L.

The ferrite crossover network is the key assembly responsible for non-reciprocal signal behavior; it controls the bandwidth and isolation properties of the circulator, which are the two key metrics associated with circulator design. To achieve high isolation and wideband operation, one attempts to adjust the geometry of the crossover traces and select the best ferrite [4], [5]. In contrast with [2], which focused on wideband performance of a standard crossover geometry, this letter considers the spiral trace geometry to obtain high isolation. Our approach is validated by both simulation and measurement data.

Instead of using the trace topology first devised by Konishi [1] and depicted in Fig. 2 (left), we seek to optimize the spiral topology of Fig. 2 (right). For this configuration, the traces on top (indicated by brown) and the traces on bottom (indicated by green) are crossing over at the center using short bond wires (indicated by red) that reduce mutual capacitance. The spiral traces tend to cover the entire surface area of the ferrite disks to enhance RF field coupling to the ferrite material and to maximize mutual inductive coupling between the traces.

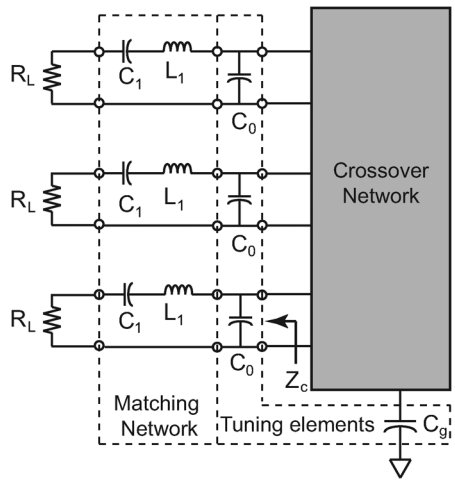

Fig. 1. Three parts of a typical circulator.

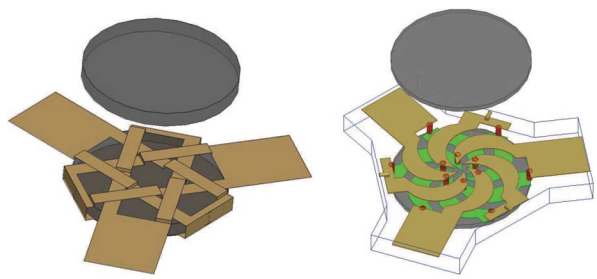

Fig. 2. Comparison of Konishi crossover trace *(left)* and novel spiral trace *(right)* topologies.

The optimization of the new trace topology is best accomplished using the notion of circulation impedance Z_c, which is defined as the load impedance that results in perfect circulation (i.e., infinite isolation, infinite return loss and zero insertion loss) for a lossless, non-reciprocal, three-port network. For a symmetrical network, Z_c is purely a function of the impedance parameters of the network such that [6]

$$Z_c = R_c + jX_c = \frac{Z_{21}^2}{Z_{31}} - Z_{11}. \tag{1}$$

The capacitances of C_g and C_0 in Fig. 1 adjust the operating frequency band of the crossover network by turning Z_c into a post-tuned impedance Z_{cp}. Then C_1, L_1 and R_L are adjusted to approximate this Z_{cp} over a band of frequencies, say from f_a to f_b. How well this is accomplished determines the actual values

Manuscript received February 11, 2013; revised March 21, 2013; accepted March 27, 2013. Date of publication April 24, 2013; date of current version June 03, 2013. This work was supported by the Office of Naval Research under grant N00014-08-1-0286.

The authors are with the Department of Electrical and Computer Engineering, University of Idaho, Moscow, ID, 83843 USA (e-mail: dong4104@vandals.uidaho.edu).

Color versions of one or more of the figures in this letter are available online at http://ieeexplore.ieee.org.

Digital Object Identifier 10.1109/LMWC.2013.2258004

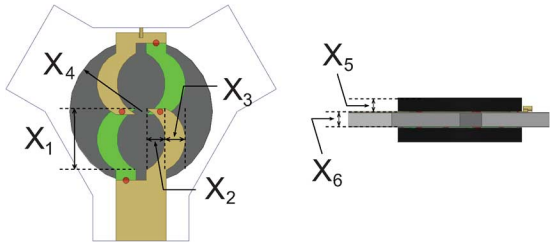

Fig. 3. Physical parameters of the spiral trace topology.

of insertion loss, return loss and isolation of the device. For our application, we seek to achieve return loss and isolation values in excess of 30 dB over the operating band.

II. Spiral Trace Design for 400 MHz Application

As shown in Fig. 3, there are six geometrical parameters that define the spiral layout (only one trace is shown for clarity)

$$\begin{aligned} X_1 &: \text{ Trace length} \\ X_2 &: \text{ Width of the spiral} \\ X_3 &: \text{ Trace width} \\ X_4 &: \text{ Ferrite disk radius} \\ X_5 &: \text{ Ferrite disk height} \\ X_6 &: \text{ PCB thickness.} \end{aligned} \tag{2}$$

Furthermore, two additional parameters define the properties of the ferrite, namely, the internal field H_o and the magnetic saturation $4\pi M_s$. These eight parameters form the optimization search space. By searching through this space with a customized optimization algorithm that uses HFSS as the kernel and by considering only components that are available in the open market, we found that the following ferrite crossover parameter set resulted in excellent device performance within the 225 to 400 MHz band:

$$\begin{aligned} X_1 &= 8.2 \text{ mm}, \quad X_2 = 2.4 \text{ mm}, \\ X_3 &= 3.5 \text{ mm}, \quad X_4 = 8.93 \text{ mm}, \\ X_5 &= 0.58 \text{ mm}, \quad X_6 = 14 \text{ mil}, \\ 4\pi M_s &= 1850 \text{ G}, \quad H_o = 142.86 \text{ Oe}. \end{aligned} \tag{3}$$

The corresponding optimized tuning capacitors are

$$C_0 = 20 \text{ pF}, \quad C_g = 168 \text{ pF}. \tag{4}$$

The Z_{cp} calculated from simulated data is shown in Fig. 4 by solid lines. For comparison, we optimized a traditional Konishi crossover network that has same ferrite disk dimension. The simulated Z_{cp} data of this crossover network are shown in Fig. 4 using dashed lines.

The improvement brought about by the spiral trace geometry over the Konishi geometry is understood by examining the two circulation impedance data sets of Fig. 4. Recall that the circulation impedance Z_{cp} ($Z_{cp} = R_{cp} + jX_{cp}$) is the load impedance needed by the post-tuned crossover network to achieve perfect circulation. Ideally, the matching network and the load R_L of Fig. 1 create an impedance Z_{Mat} (i.e., $Z_{Mat} = R_{Mat} + jX_{Mat} = R_L + j\omega L_1 + 1/j\omega C_1$) that matches Z_{cp} over a range of frequencies from f_a to f_b. Through resonance, X_{mat} produces a positive slope that matches the positive slope characteristic of X_{cp} for both the Konishi and spiral topologies, which suggests that the match between R_{cp} and R_{mat} determines device performance. Since the resistive load R_L is frequency independent, R_{cp} must also be designed to have frequency independence over the range f_a to f_b to obtain a good agreement with R_L. Clearly, the spiral geometry achieves this requirement better than the Konishi geometry when the range f_a to f_b is within the frequencies in which X_{cp} has positive slope. An elaboration on this discussion is aided using Fig. 5 by showing optimized Z_{Mat} data superimposed on Z_{cp} data of the spiral geometry. The high degree of correlation between these two data sets in the range of 255 to 345 MHz is seen and it is this correlation that produces high isolation performance. Thus, the optimization algorithm is constructed so that it chooses those designs that keep R_{cp} flat over the widest range of frequencies.

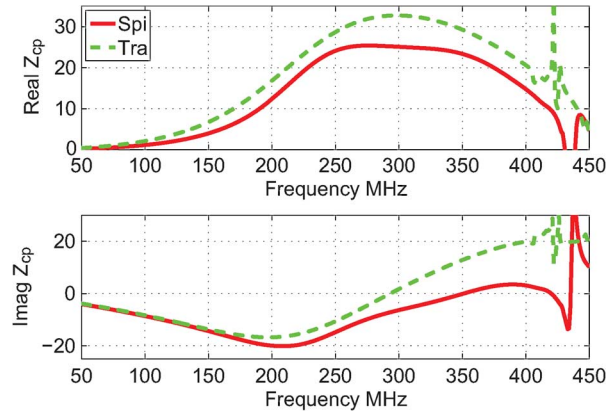

Fig. 4. Simulated Z_{cp} data comparison between spiral and traditional Konishi trace geometries.

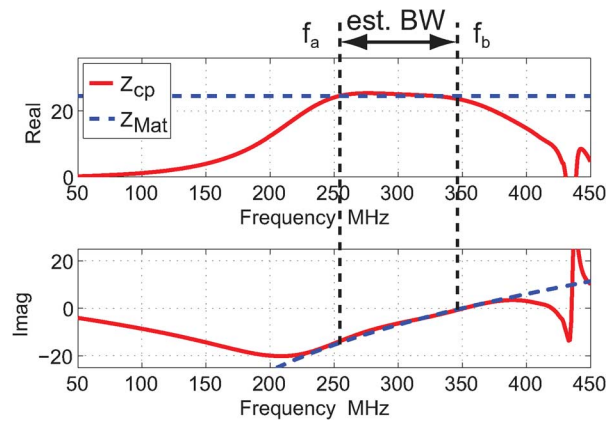

Fig. 5. Simulated data comparison of Z_{cp} and Z_{Mat}. The estimated bandwidth (BW) for high isolation is also included.

Once the trace dimensions are determined, the values of the matching network are calculated by computing the isolation and insertion loss power response of the circulator device and selecting components for which the isolation equals or exceeds 30 dB and the insertion loss is less than 0.5 dB over the frequency range 255 to 345 MHz. The resulting values are

$$R_L = 24\ \Omega, \quad C_1 = 20.3 \text{ pF}, \quad L_1 = 10.2 \text{ nH}. \tag{5}$$

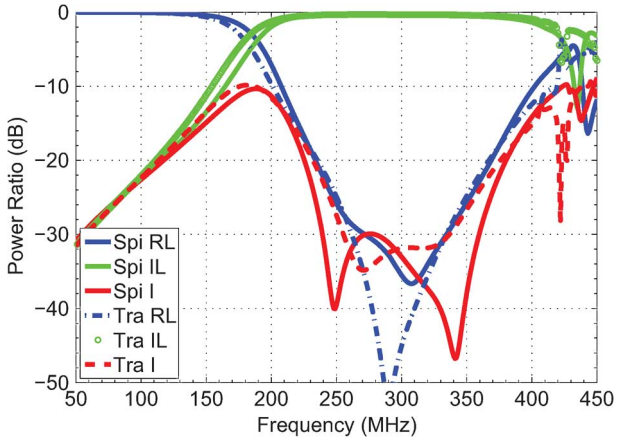

Fig. 6. Simulated frequency response comparison between the spiral trace circulator and the traditional Konishi circulator.

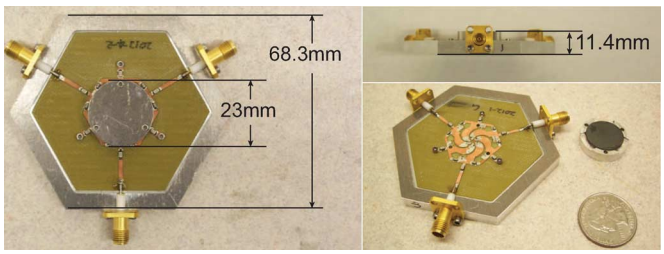

Fig. 7. Fabricated spiral trace circulator.

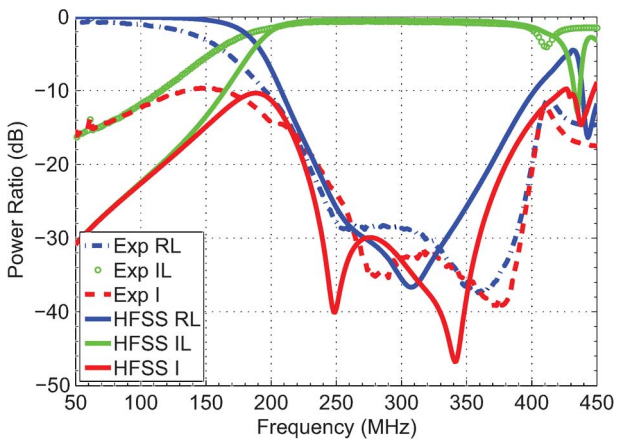

Fig. 8. Simulated and measured frequency response of spiral trace circulator for high isolation.

The simulated frequency response of the circulator device, which consists of the spiral network, tuning elements and matching network, is shown in Fig. 6 by solid lines. We see for 30 dB isolation the circulator has a bandwidth from 240 to 355 MHz, which is in agreement with the data of Fig. 5. The maximum insertion loss in this bandwidth is 0.3 dB. Also plotted in Fig. 6 is the frequency response of the Konishi crossover network used for comparison when a corresponding matching network is designed. A narrower 30 dB isolation bandwidth (260–330 MHz) is observed from the figure, which is also consistent with the prediction from the comparison data of Fig. 4.

III. Experimental Results

To verify the simulated performance of the spiral trace topology, a circulator was fabricated and measured. For the spiral trace network and tuning-elements C_0 and C_g, we used the design values from the preceding section given by (3) and (4). The ferrite disks are TTVG-1850 from Trans-Tech and an external field of 1630 Gauss is applied to force them into saturation. For the matching network and the resistive load, instead of using simulation-determined values in (5), we modified their values based on measured data of a fabricated crossover network. This is necessary since the HFSS model idealizes certain aspects of the device (e.g., homogeneous internal biasing field) to improve performance and creates ports for the lumped-element components that are not directly simulated. The modified values are

$$R_L = 17\,\Omega, \quad C_1 = 56\ \text{pF}, \quad L_1 = 3.8\ \text{nH}. \tag{6}$$

The capacitors were implemented by lumped-element components and the inductors were embedded in the transmission lines on the PCB. Pictures of the resulting device are shown in Fig. 7 and its measured frequency response is shown in Fig. 8 using dashed lines. It can be seen that a bandwidth associated with 30 dB isolation and 0.7 dB insertion loss is achieved from 260 MHz to 390 MHz. The frequency response of simulated circulator is re-plotted in Fig. 8 to show the good correlation between the measured and simulated data.

IV. Conclusion

In this letter we proposed a new spiral trace topology for the lumped-element, ferrite circulator. Using this topology, we designed a UHF circulator and achieved a deep isolation (around 30 dB), wide-band (260–390 MHz) performance. By re-optimizing the physical dimensions of the trace, the novel topology can be applied to communication systems that utilize VHF bands and possibly higher UHF bands.

References

[1] Y. Konishi, "Lumped element Y circulator," *IEEE Trans. Microw. Theory Tech.*, vol. 13, no. 6, pp. 852–864, 1965.
[2] H. Dong, J. L. Young, J. R. Smith, and B. Aldecoa, "Maximum bandwidth performance for an ideal lumped-element circulator," *Progress Electromag. Res. C*, vol. 33, pp. 213–227, 2012.
[3] R. H. Knerr and C. E. Barnes, "A compact broad-band thin-film lumped element L-band circulator," *IEEE Trans. Microw. Theory Tech.*, vol. 18, no. 12, pp. 1100–1108, 1970.
[4] Y. Konishi, "New theoretical concept for wide band gyromagnetic devices," *IEEE Trans. Magnetics*, vol. 8, no. 3, pp. 505–508, 1972.
[5] L. K. Anderson, "An analysis of broadband circulators with external tuning elements," *IEEE Trans. Microw. Theory Tech.*, vol. 15, no. 1, pp. 42–47, 1967.
[6] J. L. Young, R. S. Adams, B. O'Neil, and C. M. Johnson, "Bandwidth optimization of an integrated microstrip circulator and antenna assembly: Part 2," *IEEE Antennas Propag. Mag.*, vol. 49, no. 1, pp. 82–91, 2007.